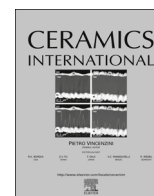




ELSEVIER

Contents lists available at ScienceDirect

Ceramics International

journal homepage: www.elsevier.com/locate/ceramint

Synthesis and enhanced photocatalytic activity of molybdenum, iron, and nitrogen triple-doped titania nanopowders



Nursev Erdogan^a, Jongee Park^b, Abdullah Ozturk^{a,*}

^a Middle East Technical University, Metallurgical and Materials Engineering Department, Ankara, Turkey

^b Atilim University, Metallurgical and Materials Engineering Department, Ankara, Turkey

ARTICLE INFO

Article history:

Received 24 June 2016

Received in revised form

18 July 2016

Accepted 22 July 2016

Available online 27 July 2016

Keywords:

Synthesis

TiO₂

Doping

Photocatalysis

Nanopowder

ABSTRACT

A novel Mo, Fe, and N triple-doped rutile TiO₂ nanopowder was synthesized with simple HNO₃ assisted hydrothermal treatment. Powders synthesized were characterized by using x-ray diffraction (XRD), x-ray photoelectron spectroscopy (XPS), inductively coupled plasma mass spectrometry (ICP-MS), scanning electron microscopy (FESEM), high resolution transmission electron microscopy (HRTEM), and Brunauer-Emmett-Teller (BET) surface area analysis techniques. Mo doping initiated the formation of a structure composed of a mixture of anatase and rutile with some modifications in morphology; but Mo, Fe, and N triple-doped titania powders are composed of entirely rutile structures. XPS analysis confirmed that Mo dissolved in the structure, replacing Ti atoms and forming some MoO₃ partially crystallized nano regions on the surface. Existence of Fe in the TiO₂ crystal lattice was confirmed by ICP analysis. Fe doping had an influence on the crystal structure and morphology. N was found to be dissolved in the co-doped structure by HNO₃ catalyzer autogenously. Methylene blue degradation testing and band gap measurements were performed by using UV-vis photospectroscopy and diffuse reflector apparatus in order to evaluate the photocatalytic performance of the powders. Dopant elements decreased band gap energy steadily. An enhanced photoactivity was reached by Mo, Fe, and N triple-doping as compared with that of undoped, and mono doped TiO₂ powders under UV-light irradiation. Possible reasons for the enhancement in photocatalytic activity are outlined.

© 2016 Elsevier Ltd and Techna Group S.r.l. All rights reserved.

1. Introduction

Titania (TiO₂) photocatalyst has received much attention since Fujishima and Honda's discovery of water splitting effect of TiO₂ under UV light [1]. Among the three polymorphs of TiO₂, anatase has been widely investigated due to its photo reactivity in catalytic applications [2–4]. In comparison to anatase TiO₂, rutile is less reactive due to its higher recombination rate of electron–hole pairs and also to a lower surface affinity for many organic compounds [5–7]. However, thermodynamically, rutile is more stable than anatase and could be more efficient in visible light induced photocatalytic processes because of the lower band gap compared to anatase [8]. Recent publications have shown that surface and morphological modifications and doping or co-doping TiO₂ with transition metals, alkaline earth elements, and non-metals improves the photocatalytic activity of rutile TiO₂ [9–13].

Among the various nonmetal dopants, nitrogen doping has been considered to be a powerful way to extend the light

adsorption of TiO₂ from the UV to the visible region [14–16]. Doping TiO₂ with 3d transitional metal ions has been investigated extensively for shifting the photo response of TiO₂ into the visible region by narrowing the band gap while inducing new intermediate energy levels [5,17]. Among various dopants, the similar radii of Mo⁶⁺ and Fe³⁺ (0.073 nm and 0.069 nm, respectively) to that of Ti⁴⁺ (0.075 nm) makes them attractive for TiO₂ doping because they would cause low or no lattice distortion. Although single element doping reduces the band gap of TiO₂ to some extent, it suffers from the existence of a carrier recombination center and the formation of strongly localized d states within the band gap, which significantly reduce carrier mobility. Thus, researchers have experimented with co-doping of metals and non-metals to increase the efficiency of TiO₂ in several studies [18–21]. Zhang et al. [22] synthesized Mo and N co-doped TiO₂ nanotubes using the anodization method, and the synergistic effect of Mo and N extended the absorption of TiO₂ nanotube arrays into the whole visible light region and resulted in remarkably enhanced photocatalytic activity for the degradation of methylene blue (MB) under visible light irradiation. Using the sol-gel method, Liu et al. [23] synthesized Mo and Fe co-doped TiO₂ nano powders, which

* Corresponding author.

E-mail address: abdullah@metu.edu.tr (A. Ozturk).

absorbed visible light, had higher separation efficiency of photo induced electrons and holes, and possessed higher photocatalytic activity compared to anatase TiO₂. Kim et al. [24] sonochemically synthesized Fe-N co-doped TiO₂ displayed enhanced photochemical behavior compared to a well-known, commercial TiO₂ powder (P25). Although there has been research on Mo and N, Mo and Fe, Fe and N co-doping strategies, no existing research has been reported on Mo-Fe-N triple-doping of TiO₂ nanopowder.

The purpose of this study was to enhance the light response and photocatalytic properties of rutile titania through Mo, Fe, and N triple-doping by hydrothermal treatment. The effect of dopants on the morphology and crystallographic properties of titania powder was also investigated. Photocatalytic activity of the Mo, Fe, and N triple-doped TiO₂ powders was evaluated in terms of the degradation of MB solution under UV-light illumination. Powders prepared were characterized to elucidate the observed enhanced photoactivity.

2. Experimental procedure

2.1. Synthesis

TiO₂ powders were synthesized through a procedure reported previously by the authors [25]. Synthesis began by diluting concentrated HNO₃ (Aldrich 70%) with distilled water to obtain 8 M HNO₃ aqua solution. Then, 10 mL of titanium tetra isopropoxide (TTIP) (Aldrich 97%) was dissolved in the freshly prepared diluted HNO₃ solution under magnetic stirring at 300 rpm for 15 min. Necessary amounts of Mo standard solution (1000 mg/L) and Fe₃(NO₃)₃·9H₂O compound were added as Mo and Fe sources, respectively, to achieve the desired Mo and Fe doping. Solutions were coded to indicate Mo and Fe contents as shown in Table 1. The resulting clear and transparent solution of 150 mL was transferred into the Teflon lined vessel of the high pressure hydrothermal reactor. The capacity of the vessel was 250 mL. Hydrothermal treatment was performed at 140 °C for 4 h.

2.2. Characterization

The structures synthesized were detected using an X-ray diffractometer (Rigaku, D/MAK/B). The phase composition, purity, and crystallinity of all the samples were identified through X-Ray diffraction (XRD) analysis in continuous scan mode at a rate of 0.03 °/s. XRD patterns were analyzed using Rigaku 4.2 software to identify the crystalline phase(s) present in the products. The same amount of powder (~0.2 g) was used for every analysis. Lattice parameters of the powders were determined using XRD data. The crystallite size of the anatase and rutile phases was calculated using Scherrer's equation from (101) reflection of anatase and (110) reflection of rutile. Size calculations were performed assuming crystallites were spherical in shape. The phase content for

all products was calculated from XRD patterns, using the following equation.

$$X_A = \left[1 + 1.26(I_R/I_A) \right]^{-1}$$

Where X_A is the fraction of anatase phase in the mixture, while I_A and I_R are the integrated intensities of the (101) reflection of anatase phase and the (110) reflection of rutile phase.

The morphologies of the structures were examined using high resolution transmission electron (HRTEM, JEM-2010, JEOL Corporation) and field emission scanning electron (FESEM, Nova Nanosem) microscopes. The operating voltage for HRTEM and for FESEM was 200 kV and 18 kV, respectively. Samples for FESEM analysis were coated with gold by sputtering method. For HRTEM analysis, powders were accumulated on carbon grid after mixing with ethanol and sonicated for maximum dispersion at 120 W for 30 min. X-ray photoelectron spectroscopy (XPS) was performed under ultrahigh vacuum at a pass energy of 93.90 eV on a Specs EA 300 system equipped with a dual X-ray source by using a Mg Kα (1253.6 eV) anode and a hemispherical energy analyzer. All binding energies were calibrated with contaminant carbon (C 1s=285 eV) as a reference. Elemental analysis was done using inductively coupled plasma mass spectrometry (ICP-MS, Perkin Elmer DRC II) in Ar. Sample preparation was accomplished by solving 50 mg powder in 200 mL HF solution. Surface area of the powders was measured using Quantachrome Corporation, Autosorb-6 by multi point Brunauer, Emmett and Teller (BET) method.

2.3. Photo-degradation of methylene blue (MB)

The diffuse reflector apparatus of the UV-vis spectrophotometer (Scinco S-3100) was used for the measurements of diffuse reflectance. White blank measurement was performed in accordance with USRS-99-010 standard. The percent reflection against wavelength graph was transformed using the Kubelka-Munk method to an [eV]^[1/2] against [eV] graph. Band gap energy of the powder sample was calculated by extrapolating the mid-section of the graph to the x axis. The effect of co-doping on photocatalytic activity was evaluated through degradation of methylene blue (MB) solution under a 100 W UV lamp with a wavelength at 365 nm and continuous stirring using a magnetic stirrer. The distance between the source and the surface of Pyrex container (300 mL capacity) was 5 cm. In order to keep the temperature of the solution constant during the reaction, water was circulated through the annulus of the jacket quartz tube. Photocatalytic tests were done using 100 mL solution. The MB concentration was 10 mg/L with a catalyst loading of 0.5 g/L. Before irradiation, the suspension aqueous solution was stirred continuously in dark for 30 min to ensure adsorption/desorption equilibrium. Initial concentration of MB before dark mixing was used as the initial value for further kinetic treatment of the photodecomposition processes to identify adsorption values. 3 mL samples taken from the solution at regular intervals using a syringe filter (Millex Millipore, 0.22 μm) were analyzed using the UV-vis spectrophotometer to determine the concentration of MB. The removal efficiency of the photocatalyst was calculated as follows:

$$\eta = (C_0 - C_t)/C_0 \times 100$$

where C₀ and C_t are the concentrations of HCHO at initial and different irradiation times, respectively.

Table 1

Sample codes, crystal structures and crystallite size values.

Sample code	Dopant amount in the source (wt%)		Weight percentage of phases (wt%)		Crystallite size of the phases (nm)	
	Mo	Fe	Anatase	Rutile	Anatase	Rutile
Mo0Fe0	0	0	55	45	6.98	8.34
Mo1Fe0	1	0	47	53	9.80	13.18
Mo2Fe0	2	0	61	39	7.27	9.51
Mo2Fe0.5	2	0.5	0	> 99	–	9.19
Mo2Fe1	2	1	0	> 99	–	10.48

Download English Version:

<https://daneshyari.com/en/article/5438728>

Download Persian Version:

<https://daneshyari.com/article/5438728>

[Daneshyari.com](https://daneshyari.com)